Chemical Papers
https://doi.org/10.1007/s11696-018-0520-9

ORIGINAL PAPER

Synthesis, evaluation and docking studies of some 4-thiazolone derivatives as effective lipoxygenase inhibitors

Sushant Kumar Shrivastava[1] · Brijesh K. Patel[1] · Prabhash Nath Tripathi[1] · Pavan Srivastava[1] · Piyoosh Sharma[1] · Avanish Tripathi[1] · Ankit Seth[1] · Manish Kumar Tripathi[1]

Received: 9 August 2017 / Accepted: 26 May 2018
© Institute of Chemistry, Slovak Academy of Sciences 2018

Abstract

Some promising 4-thiazolone derivatives as lipoxygenase inhibitors were designed, synthesized, characterized and evaluated for anti-inflammatory activity and respective ulcerogenic liabilities. Compounds (**1b**, **1e**, **3b**, and **3e**) exhibited considerable in vivo anti-inflammatory activity (57.61, 79.35, 75.00, and 79.35%) against carrageenan-induced rat paw edema model, whereas compounds (**1e**, **3b**, and **3e**) were found active against the arachidonic acid-induced paw edema model (55.38, 55.38, and 58.46%). The most potent compound (**3e)** exhibited lesser ulcerogenic liability compared to the standard diclofenac and zileuton. Further, the promising compounds (**1e** and **3e**) were evaluated for in vitro lipoxygenase (LOX; $IC_{50} = 12.98$ µM and $IC_{50} = 12.67$ µM) and cyclooxygenase (COX) inhibition assay (COX-1; $IC_{50} > 50$ µM and, COX-2; $IC_{50} > 50$ µM). The enzyme kinetics of compound **3e** was evaluated against LOX enzyme and supported by in silico molecular docking and molecular dynamics simulations studies. Overall, the results substantiated that 5-benzylidene-2-phenyl-4-thiazolones are promising pharmacophore for anti-inflammatory activity.

Keywords 4-Thiazolone · One-pot multicomponent reaction · Anti-inflammatory · Lipoxygenase

Introduction

Lipoxygenase (LOX) enzyme produces leukotrienes (LTs) and lipoxins (LXs) from arachidonic acid (AA) LT–LX metabolism. These are potent inflammatory mediators, responsible for allergic inflammation and gastric ulceration (Martel-Pelletier et al. 2003; Shrivastava et al. 2017). The LOX enzymes exist in human beings in three functional isoforms 5-, 12-, and 15-LOXs, whereas isoforms 9- and 13-LOX exist in plants (Reddy et al. 2015). The LOX enzyme generally produce 5-hydroperoxyeicosatetraenoic acid metabolites (HPETEs) by the addition of molecular oxygen into the substrate (Carter et al. 1997; Murphy and Gijón 2007; Srivastava et al. 2016), and generates inflammatory leukotrienes that regulate inflammation, pain, and fever, as well as some diverse physiological reactions such as blood flow, thrombosis, renal and gastrointestinal functions (Allaj et al. 2013). The LOX enzyme is known as non-haem iron-containing dioxygenase having an elongated active cavity without access to the bulk solvent. The enzyme is lined with both invariant amino acids (Leu368, Leu373, Leu414, Leu607 and Ile406) and LOX-specific amino acids (Ala603, Ala606, His600, and Thr364) (Gilbert et al. 2011). The reported LOX inhibitors show the interactions with amino acids through respective hydrogen bonding (His372), hydrophobic (Phe359, Leu414, Leu607, and Ala603) and electrostatic interactions. However, exploratory research is required to develop a potent molecule as a drug to clear the phase trials (Shrivastava et al. 2017).

Zileuton is the most common LOX inhibitor, frequently prescribed by physicians to treat asthma (Drazen et al. 1999), inflammation of the upper airway, and chronic obstructive pulmonary disease (COPD) (Berger et al. 2007). However, its long-term use is restricted due to side effects such as dyspepsia (Wenzel and Kamada 1996), and hepatotoxicity (Rossi et al. 2010). Therefore, to discover and develop the safe and potent LOX inhibitors devoid of toxicities is

Electronic supplementary material The online version of this article (https://doi.org/10.1007/s11696-018-0520-9) contains supplementary material, which is available to authorized users.

✉ Sushant Kumar Shrivastava
skshrivastava.phe@itbhu.ac.in

[1] Department of Pharmaceutical Engineering and Technology, Indian Institute of Technology (Banaras Hindu University), Varanasi 221 005, India

Published online: 01 June 2018

a challenge for the drug discovery and medicinal chemist in the field of pulmonary therapeutics (Zaitsu et al. 2003).

In the modern age of drug development and therapeutics, pharmacophore-based methods are successfully utilized in drug discovery over the years. Literature revealed that 4-thiazolone nucleus (Barzen et al. 2012; Hofmann et al. 2011) coupled with different aromatic moieties is proven to be effective against inflammation (Ali et al. 2007; Bekhit et al. 2010; Deep et al. 2010; Ottana et al. 2005). Taking a cue from those studies, we have explored several 4-thiazolone derivatives reported as the potential LOX inhibitors (Franke et al. 2009; Pergola and Werz 2010; Schneider et al. 2009; Scholz et al. 2009). In the design of the LOX inhibitors, the pharmacophore "5-benzylidene-2-phenyl-4-thiazolones" was equipped with two hydrogen bond acceptors, two hydrogen bond donors, and two hydrophobic groups attached to the aromatic ring (Aparoy et al. 2012; Barreiro et al. 2002) (Fig. 1).

Literature also revealed that 4-thiazolone has a poor aqueous solubility that leads to the reduced bioavailability in the central compartment. (Franke et al. 2009; Hofmann et al. 2012). Therefore, our specific aim was to design more hydrophilic as well as potent LOX inhibitors devoid of ulcerogenic liabilities. In the present study, the designed and synthesized compounds were evaluated for anti-inflammatory activity against carrageenan and arachidonic acid-induced rat paw edema models, and the active compounds were further screened through in vitro LOX, COX-1, and COX-2 enzyme inhibition assay. The enzyme kinetics was determined and collectively supported by computational molecular docking and dynamics simulations studies that were thrown light on the type of enzyme inhibition.

Experimental

Chemicals were purchased from Sigma-Aldrich (India) and used without further purification. The reaction was monitored by thin-layer chromatography on Merck silica gel 60 F254 aluminum sheets (Merck, Germany) using ethyl acetate (EtOAc):hexane (3:2) as the mobile phase. Melting points were determined using open capillary tubes on a Stuart melting point apparatus (SMP10) and are uncorrected. FT-IR spectra were recorded on Shimadzu 8400S FTIR (Shimadzu Corporation, Japan) using KBr pellets. ^{1}H-NMR (500 MHz) and ^{13}C-NMR (125 MHz) spectra were recorded on a Bruker Avance FT-NMR spectrophotometer at room temperature using TMS as an internal standard. Elemental analysis was performed on Exeter CE-440 analyzer.

Synthesis of (*Z*)-benzylidene-2-(4-chlorophenyl) thiazol-4(5H)-one derivative (1a–1e)

The substituted aromatic aldehydes (5.34 mmol) were added to the mixture of thioglycolic acid (7.89 mmol), 4-chlorobenzonitrile (5.78 mmol) and methanolic triethylamine (6.58 mmol). The reaction mixture was stirred at room temperature for 30 min and refluxed for 16–24 h. On the completion of the reaction, the solvent was evaporated under reduced pressure, and the crude product was recrystallized from methanol and washed with acetone to get the pure solid compounds **1a–1e** (Scheme 1) (Zayed et al. 1985).

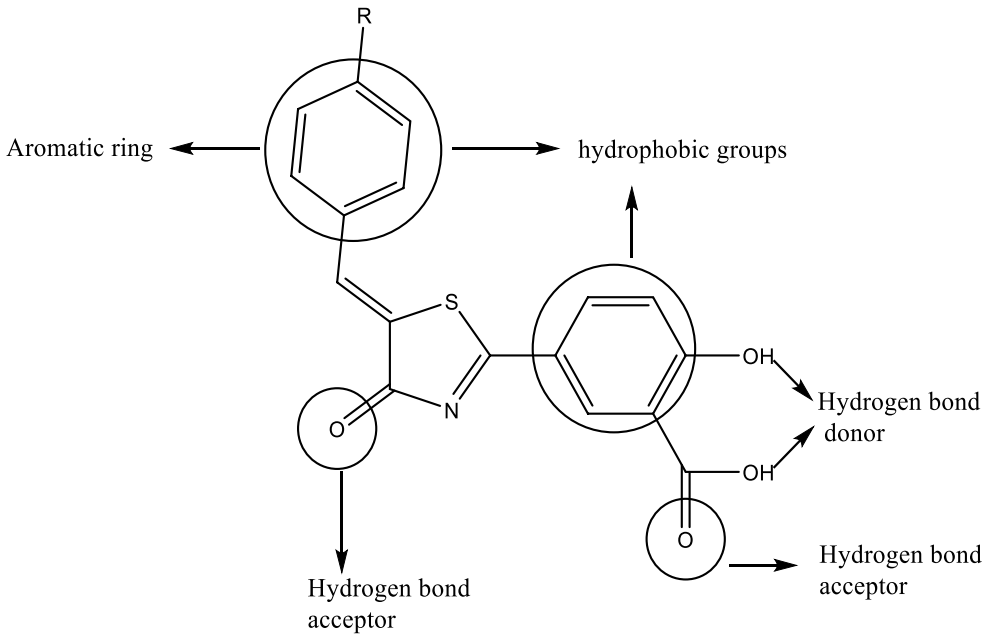

Fig. 1 Pharmacophoric consideration of designed molecule

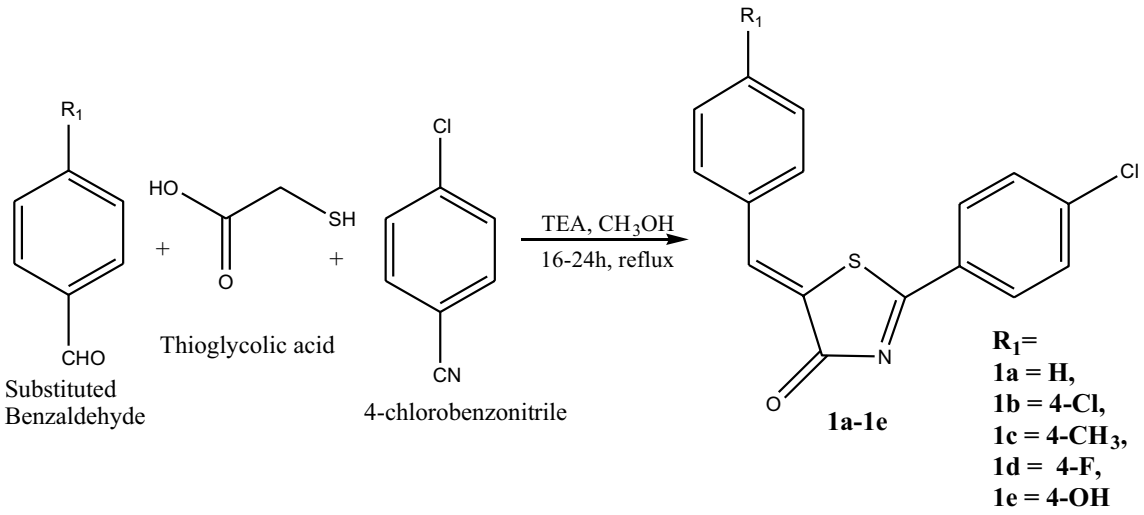

Scheme 1 Synthesis of target compounds **1a–1e**

Synthesis of 5-cyano-2-hydroxybenzoic acid (2)

Compound (**2**) was synthesized from the 5-aminosalicylic acid by the reported procedure (Qiu et al. 1999; Sandmeyer 1884).

Synthesis of (*Z*)-5-(5-benzylidene-4-oxo-4,5-dihydrothiazol-2-yl)-2-hydroxybenzoic acid (3a–3e)

The substituted aromatic aldehydes (5.34 mmol) were added to the mixture of thioglycolic acid (9.19 mmol), compound **2** (6.13 mmol), and methanolic triethylamine (7.36 mmol). The reaction mixture was stirred at room temperature for 30 min and then refluxed for 20–30 h. The reaction mixture was evaporated under reduced pressure, and the crude product was recrystallized from methanol. Further, the obtained product was washed with acetone to afford the pure crystals of compounds **3a–3e** (Scheme 2) (Zayed et al. 1985).

Physicochemical characterization

The partition coefficient (log P) of synthesized compounds (**1a–1e** and **3a–3e**) was determined using n-octanol and buffer (pH 7.4) by the shake flask method. The log *P* was calculated by correlating the absorbance with the concentration using a standard plot.

Pharmacology

Animals

In vivo studies were performed on healthy Wistar rats weighing around 200–250 gm procured from Central Animal Breeding House, Institute of Medical Sciences, Banaras Hindu University, Varanasi, India. The animals were housed at room temperature of 25 ± 2 °C, 45–55% relative humidity under 12 h light/dark cycles. Animals had free access to water ad libitum and fed with semi-synthetic balanced diet. The in vivo experimental protocol was duly approved by the Central Animal Ethical Committee of BHU, Varanasi, India (Protocol No. Dean/12-13/CAEC/18].

Acute oral toxicity study

The acute toxicity of synthesized compounds was determined as per the OECD 423 guidelines (OECD 423-2002) on healthy nulliparous female rats. Tested compounds (**1a–1e** and **3a–3e**) were well tolerated up to a dose 500 mg kg^{-1}. Also, no mortality was observed till 14 days post-administration of the test compounds. The result showed the significant safety margin of all the evaluated compounds.

Carrageenan-induced rat paw edema (acute inflammatory model)

Carrageenan-induced rat paw edema model was used as standard screening experiment to observe the acute inflammation. The paw edema was induced by sub-plantar administration of 0.1 ml of a 1% w/v lambda-carrageenan in normal saline on the left hind paw of the rats. The animals were divided into various groups along with pre-treated standard diclofenac (10 mg kg^{-1}, p.o.) and equimolar dose of test compounds (**1a–1e** and **3a–3e**) in 0.3% CMC. The vehicle was administered orally to the control group. The paw size was measured in volume (mL) using plethysmometer after 2, 4, and 6 h of the intoxication of carrageenan injection. The animals were pre-treated with the test compounds (**1a–1e**

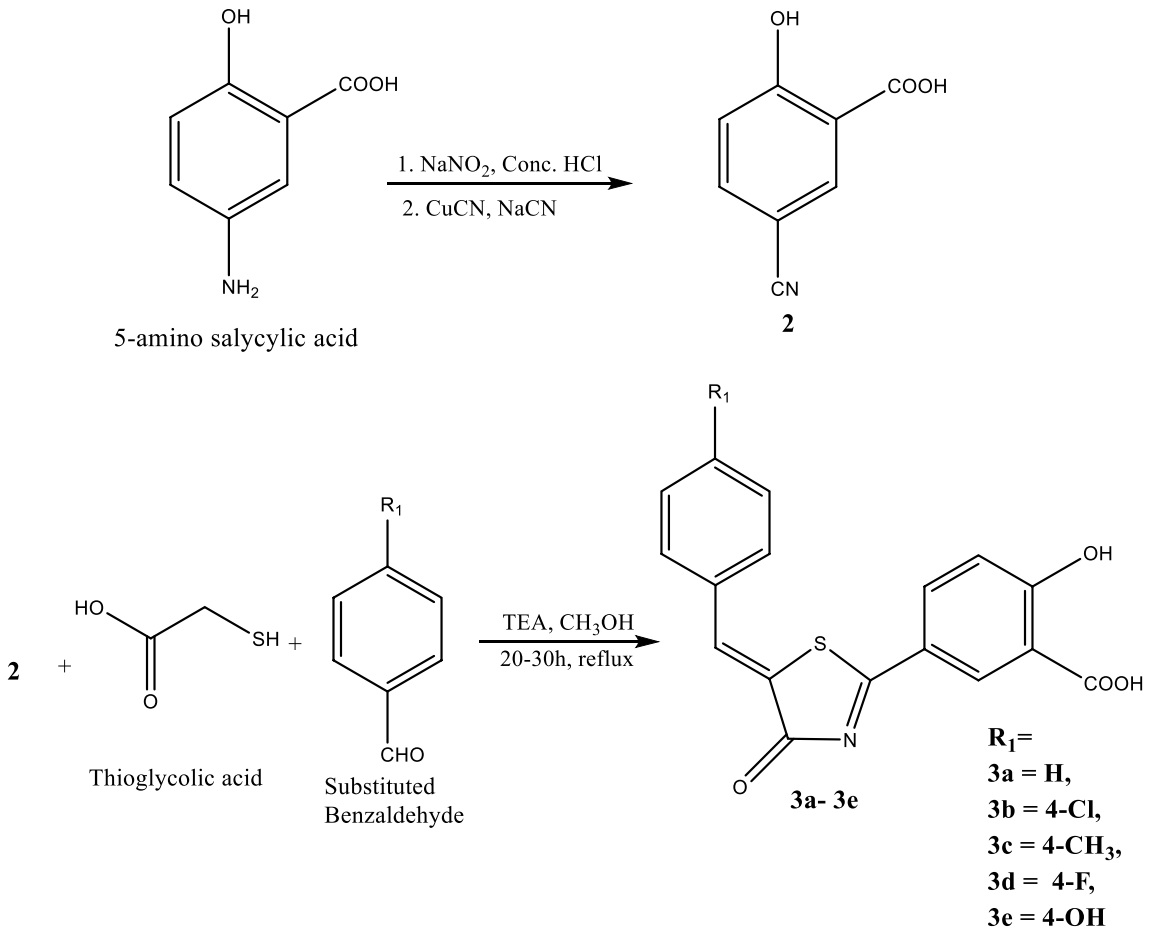

Scheme 2 Synthesis of target compounds **3a–3e**

and **3a–3e**) and standard drug 1 h before the administration of carrageenan (Winter et al. 1962).

Arachidonic acid-induced rat paw edema

AA-induced rat paw edema model was used to assess anti-inflammatory activity specific for LOX enzyme. The paw edema was induced by sub-plantar administration of 0.1 ml of 0.5% w/v AA in 0.2 M carbonate buffer (pH 8.2) on the right hind paw of rats after 30 min post-drug treatment. The 0.3% CMC was used as a control, and the test compounds were given at an equimolar dose relative to standard zileuton 10 mg kg^{-1} p.o. A digital vernier caliper measured changes in thickness (mm) after 1 h of the AA injection (DiMartino et al. 1987).

Acute ulcerogenic studies

Ulcerogenic liability of the most active compound (**3e**) and standard diclofenac was evaluated on the 21st day of the AA-induced rat paw edema bioassay. The rats were forfeited with cervical dislocation. The incision was done on the peritoneal cavity; stomach was removed, washed with distilled water, rinsed with normal saline and inspected through the 3X magnifying lens for any evidence of ulcer. Lesions were counted, and ulcer index was calculated (Banerjee et al. 2015; Szelenyi and Thiemer 1978). Further, histological studies were carried out on embedded paraffin blocks, fixed in 10% v/v formalin and stained with hematoxylin and eosin.

In-vitro COX inhibition assay

The COX-1 and COX-2 inhibitory potential of active compounds were evaluated using colorimetric COX (ovine) Inhibitor Screening Assay Kit (Cayman Chemicals; Item No. 560131). Different dilutions of celecoxib, diclofenac, and compounds (**1e** and **3e**) were incubated with the enzyme for 5 min at 25 °C. After the incubation, the substrate and AA were added, and the absorbance was recorded at 412 nm using multimode microplate reader (Pradelles et al. 1985).

In-vitro LOX inhibition assay

Soybean lipoxygenase (linoleate 13*S*-lipoxygenase) is frequently used as a dependable screen for LOX inhibition. It has been studied that AA-binding sites in soybean lipoxygenase contribute to almost the similar resemblance with animal LOX enzyme (Tsurumi et al. 1986). The assay was performed according to continuous spectrophotometric rate determination method. The stock solution of lipoxygenase was prepared by dissolving 5000–10,000 units/ml of lipoxidase in 200 mM borate buffer at pH 9.0. Further, inhibitors (**1e** and **3e**) in six different concentrations range of 0.025–50 µM were selected and used for determination of the enzyme inhibition activity. Increasing concentrations of inhibitors were added to the enzyme solution and kept for 5 min followed by the substrate addition. The resulting solution was incubated at room temperature for 20 min with continuous shaking. The enzyme–substrate reaction was considered maximum in the vehicle due to the formation of enzyme–substrate (ES) complex. Blank contains all the substances except the enzyme solution to account for non-enzymatic reactions. The concentration of each test compound was recorded in triplicates at 234 nm using multimode microplate reader, and their IC_{50} values were determined graphically from absorption v/s concentration curve (Banerjee et al. 2016).

Enzyme kinetic studies

Continuous spectrophotometric rate determination method was used to identify the type of enzyme inhibition by the compound (**3e**). The different concentrations of substrate (AA) were prepared in Tween-20 in 200 mM borate buffer at pH 9.0. The fixed concentration of LOX enzyme (10,000 units/ml) was prepared in 200 mM borate buffer at pH 9.0. The enzyme kinetics was analyzed at the different concentrations of the substrate either in the absence or presence of compound (**3e**). The enzyme kinetics was studied by Lineweaver and Burk method (Lineweaver and Burk 1934).

Computational studies

Molecular docking study

The synthesized compounds (**1e** and **3e**) were computationally docked into the LOX enzyme pockets (PDB Code: 3V99) using Glide XP module (Schrodinger, LLC, USA, 2016-1 Maestro 10.5.014) to gain structural insights of binding of a ligand to the enzyme. The crystal structure of the enzyme–substrate complex was retrieved from the protein data bank and used for molecular docking. The enzyme was optimized with the "protein preparation wizard" workflow. The co-crystallized ligand was extracted, and the ligand-binding site was defined using Glide Grid Generation module. The ligands were built-up using LigPrep module application through the OPLS2005 force field. OPLS stands for optimized potential liquid simulations that give the corresponding minimum energy conformers of the ligands. The default settings were used for all other parameters to perform the docking simulations.

Molecular dynamics simulations

Molecular dynamics simulations confirmed the binding mode and conformational stability of compound (**3e**) on LOX enzyme. Desmond package incorporated in Schrodinger Maestro 10.5.014 program using OPLS-AA force field was used to predict the thermodynamic stability of the protein–ligand system. Simulations were performed by placing the docked complex (**3e** + LOX enzyme) in predefined TIP3 water and orthorhombic periodic boundary condition. Initially, the volume of periodic box condition was calculated as 750,210 $Å^3$ and was minimized to 716,092 $Å^3$. The solvated system was neutralized with the addition of 18 Na^+ counterions. The system was reduced to 2000 steps and relaxed using the default protocols. Molecular dynamics simulations were carried out at normal volume, and temperature and pressure were kept at 300 K and 1 atmospheric pressure. Finally, the system was allowed to run for 50 ns time scale and trajectories were recorded at 5 ps interval.

In-silico ADME studies

The QikProp module of Schrodinger Maestro 10.5.014 Release 2016-1 was used to predict the ADME properties of the active compound **3e** and standards (**zileuton**, **C06**, and **ST1098**). It predicts the pharmaceutically relevant properties of the compounds along with several descriptors. Ligands were initially neutralized and used for the QikProp analysis. The program was processed in a normal mode to observe the physiological properties including the total solvent accessible surface area (SASA), Van der Waals surface area of polar nitrogen and oxygen atoms (PSA), hydrogen bond donor, hydrogen bond acceptor, predicted hexadecane/gas partition coefficient (QPlogPC16), Predicted octanol/gas partition coefficient (QPlogPoct), and predicted octanol/water partition coefficient (QPlogPo/w).

Results and discussion

Chemistry and spectral characterization

The 4-thiazolone derivatives were designed by substituting more polar groups such as hydroxyl on 5-benzylidene-4-thiazolone moieties for improving hydrophilic characteristics.

Table 1 Results of spectral characterization

Compound	Spectral data
1a	FT-IR, cm^{-1}: 1664 (>C=O), 1564 (>C=N) ^{1}H-NMR (DMSO-d_6, 500 MHz), δ: 8.20 (d, J = 8.0 Hz, 2H, Cl-Ph-3,5H), 8.01 (s, 1H, –CH=), 7.64 (d, J = 8.5 Hz, 2H, Cl-Ph-2,6H), 7.55–7.24 (m, 5H, benzylidene). ^{13}C-NMR (DMSO-d_6, 125 MHz), δ: 185.4 (thia-4C), 183.1 (thia-2C), 140.0 (thia-5C), 138.2 (Cl-Ph-2,6C), 138.1 (Cl-Ph-1C), 132.3 (benzylidene-4C), 131.2 (–CH=), 131.0 (Cl-Ph-3,5C), 129.5 (Cl-Ph-4C), 128.0 (benzylidene-2,6C), 127.3 (benzylidene-1C), 126.2 (benzylidene-3,5C).
1b	FT-IR, cm^{-1}: 1681 (>C=O), 1593 (>C=N) ^{1}H-NMR (DMSO-d_6, 500 MHz), δ: 8.23 (d, J = 8.5 Hz, 2H, Cl-Ph-3,5H), 8.07 (s, 1H, –CH=), 7.84 (d, J = 7.5 Hz, 2H, Cl-benzylidene-2,6H), 7.77 (d, J = 8.0 Hz, 2H, Cl-benzylidene-3,5H), 7.67 (d, J = 8.0 Hz, 2H, Cl-Ph-2,6H). ^{13}C-NMR (DMSO-d_6, 125 MHz), δ: 184.1 (thia-4C), 182.1 (thia-2C), 140.3 (thia-5C), 139.8 (Cl-Ph-2,6C), 138.1 (Cl-Ph-1C), 135.3 (Cl-benzylidene-1C), 132.4 (–CH=), 130.7 (Cl-benzylidene-2,6C), 130.3 (Cl-benzylidene-4C), 130.2 (Cl-Ph-3,5C), 129.5 (Cl-Ph-4C), 128.5 (Cl-benzylidene-3,5C).
1c	FT-IR, cm^{-1}: 1675 (>C=O), 1591 (C=N) ^{1}H-NMR (DMSO-d_6, 500 MHz), δ: 7.93 (s, 1H, –CH=), 7.78 (d, J = 8.0 Hz, 2H, Cl-Ph-3,5H), 7.65 (d, J = 8.0 Hz, 2H, Cl-Ph-2,6H), 7.45 (d, J = 8.2 Hz, 2H, CH_3-benzylidine-3,5), 7.12 (d, J = 8.0 Hz, 2H, CH_3-benzylidene-2,6H), 2.65 (s, 3H, –CH_3-Ph). ^{13}C-NMR (DMSO-d_6, 125 MHz), δ: 185.1 (thia-4C), 182.2 (thia-2C), 141.1 (thia-5C), 139.1 (Cl-Ph-1C), 137.2 (CH_3-benzylidene-1C), 131.1 (–CH=), 130.2 (Cl-Ph-3,5C), 130.1 (CH_3-benzylidene-3,5C), 129.8 (Cl-Ph-4C), 129.7 (Cl-Ph-2,6C), 129.1 (CH_3-benzylidene-4C), 131.0 (CH_3-benzylidene-2,6C), 22.1 (–CH_3).
1d	FT-IR, cm^{-1}: 1664 (>C=O), 1592 (>C=N) ^{1}H-NMR (DMSO-d_6, 500 MHz), δ: 8.23-7.98 (m, 3H, *F*-benzyledine-3,5H and –CH=), 7.78 (d, J = 8.5 Hz, 2H, Cl-Ph-3,5H), 7.68 (d, J = 8.0 Hz, 2H, Cl-Ph-2,6H), 7.30 (d, $J_{H,H}$ = 8.4 Hz, $J_{H,F}$ = 8.9 Hz, 2H, *F*-benzyledine-2,6H). ^{13}C-NMR (DMSO-d_6, 125 MHz), δ: 184.7 (thia-4C), 182.3 (thia-2C), 167.1 ($J_{C,F}$ = 249.0 Hz, F-benzylidene-1C), 139.0 (thia-5C), 139.4 (Cl-Ph-1C), 131.1 (–CH=), 131.2 (($J_{C,F}$ = 8.6 Hz, *F*-benzylidene-3,5C), 130.2 (Cl-Ph-3,5C), 129.7 (Cl-Ph-2,6C), 129.8 (Cl-Ph-4C), 127.8 ($J_{C,F}$ = 3.5 Hz, *F*-benzylidene-4C), 116.7 ($J_{C,F}$ = 23.2 Hz, *F*-benzylidene-2,6C).
1e	FT-IR, cm^{-1}: 3163 (-OH), 1664 (>C=O), 1597 (>C=N) ^{1}H-NMR (DMSO-d_6, 500 MHz), δ: 10.53 (s, 1H, –OH), 8.19 (d, J = 8.0 Hz, 2H, HO-benzylidene-3,5H), 7.97 (s, 1H, –CH=), 7.75 (d, J = 8.5 Hz, 2H, Cl-Ph-3,5H), 7.69 (d, J = 8.0 Hz, 2H, Cl-Ph-2,6H), 6.96 (d, J = 8.5 Hz, 2H, HO-benzylidene-2,6H). ^{13}C-NMR (DMSO-d_6, 125 MHz), δ: 184.4 (thia-4C), 182.1 (thia-2C), 161.1 (HO- benzylidene-1C), 140.0 (thia-5C), 139.0 (Cl-Ph-1C), 133.4 (–CH=), 130.1 (Cl-Ph-3,5C), 130.0 (Cl-Ph-2,6C), 129.8 (Cl-Ph-4C), 124.3 (HO-benzylidene-4C), 121.8 (HO-benzylidene-3,5C), 116.6 (HO-benzylidene-2,6C).
2	FT-IR, cm^{-1}: 3458 (–OH), 2235 (–CN), 1685 (>C=O, –COOH) ^{1}H-NMR (DMSO-d_6, 500 MHz), δ: 8.14 (s, 1H, Ph-6H), 7.85 (d, J = 8.5 Hz 1H, Ph-4H), 7.06 (d, J = 9.0 Hz 1H, Ph-3H). ^{13}C NMR (DMSO-d_6, 125 MHz), δ: 169.9 (>C=O, –COOH), 164.8 (Ph-2C), 137.9 (Ph-4C), 135.1 (Ph-6C), 118.7 (Ph-3C), 118.6 (Ph-1C), 115.6 (–CN), 100.8 (Ph-5C).
3a	FT-IR, cm^{-1}: 3365 (–COOH), 3028 (Ph-H), 1684, 1657 (>C=O), 1591 (–C=N) ^{1}H-NMR (DMSO-d_6, 500 MHz), δ: 10.40 (s, 1H, –COOH), 8.35 (d, J = 2.5 Hz, 1H, COOH-Ph-6H), 7.87 (s, 1H, –CH =), 7.71 (d, J = 3.0 Hz, 1H, COOH-Ph-4H), 7.54 (d, J = 7.5 Hz, 2H, benzylidene-3,5H), 7.21–7.45 (m, 3H, benzylidene-1,2,6H), 6.89 (d, J = 8.5 Hz,1H,COOH-Ar-3H), ^{13}C-NMR (DMSO-d_6, 125 MHz), δ: 185.4 (thia-4C), 182.0 (thia-2C), 169.0 (–COOH), 162.4 (HO-Ph-2C), 140.0 (thia-5C), 135.1 (HO-Ph-4C), 128.2 (benzylidene-1C), 135.4 (HO-Ph-6C), 131.8 (–CH =), 130.2 (benzylidene-4C), 127.5 (benzylidene-2,6C), 126.5 (benzylidene-3,5C), 125.2 (HO-Ph-5C), 118.3 (HO-Ph-3C), 116.0 (HO-Ph-1C).
3b	FT-IR, cm^{-1}: 3365 (–COOH), 3039 (Ph-H), 1681, 1668 (>C=O), 1555 (–C=N) ^{1}H-NMR (DMSO-d_6, 500 MHz), δ: 10.39 (s, 1H, –COOH), 8.35 (d, J = 2.5 Hz, 1H, COOH-Ph-6H), 7.89 (s, 1H, –CH=), 7.78 (d, J = 8.5 Hz, 2H, Cl-benzylidene-3,5H), 7.70 (d, J = 2.5 Hz, 1H, COOH-Ph-4H), 7.58 (d, J = 8.5 Hz, 2H, Cl-benzylidene-2,6H), 6.80 (d, J = 8.5 Hz, 1H, COOH-Ph-3H). ^{13}C-NMR (DMSO-d_6, 125 MHz), δ: 185.2 (thia-4C), 183.1 (thia-2C), 168.9 (–COOH), 162.1 (HO-Ph-2C), 139.2 (thia-5C), 136.4 (HO-Ph-4C), 136.1 (Cl-benzylidene-1C), 135.1 (HO-Ph-6C), 132.0 (–CH=), 130.2 (Cl-benzylidene-4C), 130.6 (Cl-benzylidene-2,6C), 129.0 (Cl-benzylidene-3,5C), 124.2 (HO-Ph-5C), 118.4 (HO-Ph-3C), 117.0 (HO-Ph-1C).
3c	FT-IR, cm^{-1}: 3440 (–COOH), 3039 (Ar–H), 1685, 1664 (>C=O), 1561 (–C=N). ^{1}H-NMR (DMSO-d_6, 500 MHz), δ: 10.39 (s, 1H, –COOH), 8.35 (d, J = 3.0 Hz, 1H, COOH-Ph-6H), 7.74 (s, 1H, –CH=), 7.71 (d, J = 2.5 Hz, 1H, COOH-Ph-4H), 7.33 (d, J = 8.0 Hz, 2H, CH_3-benzylidene-3,5H), 7.15 (d, J = 8.5 Hz, 2H, CH_3-benzylidene-2,6H), 6.85 (d, J = 8.5 Hz, 1H, COOH-Ar-3H), 2.74 (s, 3H, –CH_3-Ar). ^{13}C-NMR (DMSO-d_6, 125 MHz), δ: 184.8 (thia-4C), 182.2 (thia-2C), 168.2 (–COOH), 162.0 (HO-Ph-2C), 141.2 (thia-5C), 136.9 (CH_3-benzylidene-1C), 135.8 (HO-Ph-4C), 135.0 (HO-Ph-6C), 131.2 (–CH=), 130.8 (CH_3-benzylidene-2,6C), 130.2 (CH_3-benzylidene-3,5C), 128.9 (CH_3-benzylidene-4C), 124.2 (HO-Ph-5C), 118.7 (HO-Ph-1C), 117.5 (HO-Ph-3C), 22.9 (CH_3-Ph).

Table 1 (continued)

Compound	Spectral data
3d	FT-IR, cm^{-1}: 3441 (–COOH), 3041 (Ph-H), 1677, 1664 (>C=O), 1561.41 (–C=N) ^{1}H-NMR (DMSO-d_6, 500 MHz), δ: 10.34 (s, 1H, –COOH), 8.48 (d, J = 2.5 Hz, 1H, COOH-Ph-6H), 7.99 (d, J = 2.5 Hz, 1H, COOH-Ph-4H), 7.79 (s, 1H, –CH=), 7.73 (d, $J_{H,H}$ = 8.5 Hz, $J_{H,F}$ = 5.8 Hz, 2H, *F*-benzylidene-3,5H), 7.35 (d, $J_{H,H}$ = 8.0 Hz, $J_{H,F}$ = 9.1 Hz, 2H, *F*-benzylidene-2,6H), 6.77 (d, J = 8.5 Hz, 1H, COOH-Ar-3H). ^{13}C-NMR (DMSO-d_6, 125 MHz), δ: 184.8 (thia-4C), 182.6 (thia-2C), 169.7 (–COOH), 167.2 ($J_{C,F}$ = 246.2 Hz, *F*-benzylidene-1C), 161.7 (HO-Ph-2C), 138.1 (thia-5C), 136.5 (HO-Ph-4C), 134.8 (HO-Ph-6C), 131.0 (–CH=), 128.0 ($J_{C,F}$ = 3.5 Hz, *F*-benzylidene-4C), 125.2 (HO-Ph-5C), 130.7 ($J_{C,F}$ = 7.7 Hz, *F*-benzylidene-3,5C), 118.2 (HO-Ph-3C), 118.4 (HO-Ph-1C), 116.6 ($J_{C,F}$ = 22.8 Hz, *F* benzylidene-2,6 C).
3e	FT-IR, cm^{-1}: 3416, 3363 (–OH), 3066 (Ph-H), 1629 (>C=O), 1566 (–C=N). ^{1}H-NMR (DMSO-d_6, 500 MHz), δ: 10.35 (s, 1H, –COOH), 8.48 (d, J = 2.5 Hz, 1H, COOH-Ph-6H), 8.01 (d, J = 2.5 Hz, 1H, COOH-Ph-4H), 7.77 (s, 1H, –CH=), 7.65 (d, J = 8.5 Hz, 2H, HO-benzylidene-3,5H), 6.95 (d, J = 8.5 Hz, 2H, HO-benzylidene-2,6H), 6.74 (d, J = 9.0 Hz, 1H, COOH-Ph-3H). ^{13}C-NMR (DMSO-d_6, 125 MHz), δ: 185.0 (thia-4C), 182.6 (thia-2C), 169.7 (–COOH), 161.7 (HO-Ph-2C), 161.2 (HO-benzylidene-1C), 139.9 (thia-5C), 136.5 (HO-Ph-4C), 134.8 (HO-Ph-6C), 132.9 (–CH=), 125.0 (HO-Ph-5C), 124.4 (HO-benzylidene-4C), 122.2 (HO-benzylidene-3,5 C), 118.3 (HO-Ph-3 C), 118.2 (HO-Ph-1C), 116.4 (HO-benzylidene-2,6 C).
C06	^{1}H-NMR (DMSO-d_6, 500 MHz), δ: 8.12 (d, J = 8.0 Hz, 2H, CH_3-Ph-3,5H), 8.02 (s, 1H, –CH=), 7.66 (d, J = 8.5 Hz, 2H, CH_3O-benzyledine-3,5),7.37 (d, J = 8.0 Hz, 2H, CH_3-Ph-2,6H), 7.03 (d, J = 8.5 Hz, 2H, CH_3O-benzylidene-2,6H), 3.91 (s, 3H, -OCH_3-Ph), 2.49 (s, 3H, –CH_3-Ph). ^{13}C-NMR (DMSO-d_6, 125 MHz), δ: 186.4 (thia-4C), 183.6 (thia-2C), 161.9 (CH_3O-benzylidene-1C), 146.3 (thia-5C), 138.1 (CH_3-Ph-1C), 132.7 (CH_3-Ph-3,5C), 129.9 (CH_3-Ph-2,6C), 129.3 (–CH=), 128.8 (CH_3O-benzylidene-3,5C), 126.3 (CH_3-Ph-4C), 123.7 (CH_3O-benzylidene-4C), 114.8 (CH_3O-benzylidene-2,6C), 55.5 (–OCH_3), 21.9 (–CH_3).
ST1098	^{1}H-NMR (DMSO-d_6, 500 MHz), δ: 8.16 (d, J = 8.5 Hz, 2H, Cl-Ph-3,5H), 8.05 (s, 1H, –CH=), 7.66 (d, J = 9.0 Hz, 2H, CH_3O-benzyledine-3,5), 7.55 (d, J = 8.5 Hz, 2H, Cl-Ph-2,6H), 7.04 (d, J = 8.5 Hz, 2H, CH_3O-benzylidene-2,6H), 3.91 (s, 3H, –OCH_3-Ph). ^{13}C-NMR (DMSO-d_6, 125 MHz), δ: 185.1 (thia-4C), 183.2 (thia-2C), 162.2 (CH_3O-benzylidene-1C), 141.3 (thia-5C), 139.1 (Cl-Ph-1C), 132.9 (Cl-Ph-3,5C), 130.4 (–CH=), 129.8 (Cl-Ph-2,6C), 129.3 (CH_3O-benzylidene-3,5C), 126.3 (Cl-Ph-4C), 123.9 (CH_3O-benzylidene-4C), 114.9 (CH_3O-benzylidene-2,6C), 55.5 (–OCH_3).

Apart from the substituted hydroxyl group at 4th position, some lipophilic compounds have been developed by substituting methyl, chloro, and fluoro groups at the same position on 5-benzylidene. In the same way, more hydrophilic compounds were also developed by placing *O*-hydroxybenzoic acid at 2nd position of 4-thiazolones.

The 4-thiazolone derivatives (**1a–1e** and **3a–3e)** were synthesized by reacting of thioglycolic acid with 4-chlorobenzonitrile and substituted benzaldehyde through one-pot multicomponent reaction (Zayed et al. 1985). The thioglycolic acid and 4-chlorobenzonitrile were reacted in ethanol with triethylamine to get the 4-thiazolone core which was then condensed in situ with substituted benzaldehyde under the refluxed condition to generate the 4-thiazolone derivatives (**1a–1e**) (Scheme 1). The FT-IR spectra of compounds (**1a–1e**) showed distinctive stretching bands for carbonyl group >C=O in the range of 1682–1664 cm^{-1}, (–C=CH–) of a benzylidene at 1478–1425 cm^{-1} and (–C=N) of a 4-thiazolone nucleus at 1597–1555 cm^{-1}. Compound (**1e**) displayed a characteristic hydroxyl (–OH) stretching band at 3163 cm^{-1}. The ^{1}H-NMR of (**1e)** showed broad singlet proton peak at 10.53 ppm of a phenolic hydroxyl group and (–C=CH–) proton of a benzylidene at around of 8.07 ppm. The ^{13}C-NMR peak of the carbonyl group (>C=O) was observed between 185.4 and 184.1 ppm, and imine (>C=N) peak in the range of 182.6–182.0 ppm. The *p*-hydroxybenzylidene (HO-benzylidene-1C) displayed a peak at 161.1 ppm.

Further, the nitrosation of 5-aminosalicylic acid with nitrous acid (in situ from sodium nitrite and hydrochloric acid) leads to diazonium salts, and subsequent substitution of a cyanide nucleophile (–CN) under copper (I) cyanide catalysis generated the 5-cyano-2-hydroxy benzoic acid (**2**) (Sandmeyer reaction) with the removal of nitrogen gas. The FT-IR spectrum confirmed its structure, eliciting an original strong stretching band of nitrile group (–CN) at 2235 cm^{-1}, and (>C=O) of carboxylic acid at 1685 cm^{-1}. The ^{13}C-NMR exhibited a unique up-field value of phenyl-1C containing carboxylic acid, cyano (–CN) and cyano-attached carbon (phenyl-5C) at 118.6, 115.6, 100.8 ppm, respectively.

The 4-thiazolone derivatives (**3a–3e**) were synthesized by reacting thioglycolic acid, 5-cyano-2-hydroxybenzoic acid (**2**) and substituted aromatic benzaldehyde to generate the 4-thiazolone compounds (Scheme 2). The FT-IR spectra of derivatives (**3a–3e**) exhibited characteristic stretching bands for carbonyl (>C=O) groups of carboxylic acid between 1684 and 1670 cm^{-1}, (–OH) of carboxylic acid at 3365–3340 cm^{-1} and imine (–C=N) appeared in the range of 1591–1555 cm^{-1}. The ^{1}H-NMR of compounds (**3a–3e**) showed one proton peak at ~ 10.4 ppm for a carboxylic acid (–OH). The ^{13}C-NMR peak of carbonyl (>C=O) of carboxylic acid was observed at 169.7–168.2 ppm,

Table 2 Results of physical characterization and elemental analysis

Compound	Formula (*Mr*)	w_i(calc.)/% w_i(found)/%			R_f^a	Yield (%)	M.P.[b]	Log P[c]
		C	H	N				
1a[#]	$C_{16}H_{10}ClNOS$ 299.02	64.11 64.35	3.36 3.35	4.67 4.68	0.55	45	273–275	3.93
1b	$C_{16}H_9Cl_2NOS$ 334.22	57.50 57.30	2.71 2.72	4.19 4.20	0.35	38	279–281	4.21
1c	$C_{17}H_{12}ClNOS$ 313.80	65.07 65.30	3.85 3.84	4.46 4.44	0.42	34	315–317	4.32
1d	$C_{16}H_9ClFNOS$ 317.77	60.48 60.47	2.85 2.86	4.41 4.40	0.45	43	253–255	4.40
1e*	$C_{16}H_{10}ClNO_2S$ 315.77	60.86 61.10	3.19 3.53	4.44 4.91	0.32	37	345–347	4.07
2	$C_8H_5NO_3$ 163.13	58.90 59.14	3.09 3.07	8.59 8.56	–	65	–	–
3a	$C_{17}H_{11}NO_4S$ 325.34	62.76 62.01	3.41 3.42	4.31 4.30	0.45	29	286–288	3.11
3b	$C_{17}H_{10}ClNO_4S$ 359.78	56.75 56.61	2.80 2.79	3.89 3.88	0.18	40	272–274	3.36
3c	$C_{18}H_{13}NO_4S$ 339.37	63.71 63.90	3.86 3.87	4.13 4.14	0.51	24	303–305	3.59
3d	$C_{17}H_{10}FNO_4S$ 343.03	59.47 59.48	2.94 2.95	4.08 4.10	0.58	31	242–244	2.98
3e	$C_{17}H_{11}NO_5S$ 341.34	59.82 59.98	3.25 3.56	4.10 4.24	0.53	21	357–359	3.72
C06	$C_{18}H_{15}NO_2S$ 309.38	69.88 69.81	4.89 4.90	4.53 4.49	0.44	62	222–224	4.40
ST1098	$C_{17}H_{12}ClNO_2S$ 329.80	61.91 61.95	3.67 3.59	4.25 4.29	0.41	66	186–188	4.52

[#]Liang et al. Liang et al. 2016

[*]Hofmann et al. Hofmann et al. 2008

[a]Solvent system: EtOAc:hexane (3:2)

[b]Melting points were determined using open capillary tubes on a Stuart melting point apparatus (SMP10) and were uncorrected

[c]Log *P* values were determined using shake flask method

whereas the carbonyl (>C=O) of the 4-thiazolone nucleus at around 185.4–184.8 ppm, and imine (–C=N) in range 182.6–182.0 ppm. These spectral data confirmed the presence of carbonyl groups, a hydroxyl group, benzylidene group and carboxylic acid in 4-thiazolone derivatives. Spectral characterization of all derivatives by FT-IR, ^{1}H-NMR, and ^{13}C-NMR is summarized in Table 1. The results of the elemental analyses were within ± 0.4% of theoretical values. These thiazolones were further subjected to physiochemical characterization (Table 2).

Pharmacology

In the literature, 4-thiazolone compound (*Z*)-5-(4-methoxybenzylidene)-2-(*p*-tolyl)thiazol-4(5H)-one (**C06**) was reported as potential LOX inhibitor on the cellular assay, but its in vivo anti-inflammatory activity and ulcerogenic liability remain unexplored till this date. This was also the fact that compound **C06** could not achieve the desired plasma and tissue concentration due to poor aqueous solubility (Hofmann et al. 2012). In the present work, we have explored the anti-inflammatory activity of synthesized compound (**1a–1e** and **3a–3e**) against the carrageenan and AA-induced rat paw edema model for assessing the contribution of mediators involved in vascular changes associated with acute inflammation. The ulcerogenic liability was also observed to establish the gastrointestinal toxicity profile.

Carrageenan-induced rat paw edema

Carrageenan-induced rat paw edema model is frequently used for evaluation of the acute inflammatory response generated by cyclooxygenase (COX) enzyme. The progression of the carrageenan-induced hind paw edema by injection

Table 3 Paw volume and % inhibition as calculated by carrageenan-induced rat paw edema model

Compound	[a]Mean protection (% inhibition)		
	2 h	4 h	6 h
Control	0.63 ± 0.03	0.86 ± 0.04	0.92 ± 0.06
Diclofenac	0.19 ± 0.01 (69.84)	0.14 ± 0.01 (83.72)	0.12 ± 0.01 (86.96)
1a	0.43 ± 0.03 (31.75)	0.46 ± 0.03 (46.51)	0.49 ± 0.03 (46.74)
1b	0.32 ± 0.02 (49.21)	0.30 ± 0.02 (65.12)	0.39 ± 0.02 (57.61)
1c	0.39 ± 0.03 (38.10)	0.38 ± 0.02 (55.81)	0.37 ± 0.02 (59.78)
1d	0.41 ± 0.03 (34.92)	0.41 ± 0.03 (52.32)	0.42 ± 0.03 (54.35)
1e	0.24 ± 0.02 (61.90)	0.22 ± 0.01 (74.42)	0.19 ± 0.02 (79.35)
3a	0.39 ± 0.03 (38.10)	0.35 ± 0.02 (59.30)	0.33 ± 0.02 (64.13)
3b	0.27 ± 0.02 (57.14)	0.24 ± 0.02 (72.09)	0.23 ± 0.02 (75.00)
3c	0.36 ± 0.03 (42.86)	0.31 ± 0.02 (63.95)	0.39 ± 0.03 (57.61)
3d	0.44 ± 0.04 (30.16)	0.42 ± 0.03 (51.16)	0.43 ± 0.01 (53.26)
3e	0.22 ± 0.02 (65.08)	0.20 ± 0.02 (76.74)	0.19 ± 0.02 (79.35)

All other compounds were administered at an equimolar oral dose relative to 10 mg kg^{-1} diclofenac

Control 0.3% carboxymethylcellulose sodium (CMC) solution in distilled water (10 ml/kg/p.o.), *Standard* diclofenac (10 mg kg^{-1} p.o) in 0.3% CMC solution

[a]Mean protection was expressed as (%) edema inhibition of the tested compounds relative to (%) edema inhibition of standard

of lambda-carrageenan in the rat is a biphasic event. The early phase (1–2 h) releases pro-inflammatory agents such as histamine and serotonin, whereas the later stage (post-3-h treatment) release prostaglandins (Winter et al. 1962).

The anti-inflammatory activity of the 4-thiazolone compounds (**1a–1e** and **3a–3e**) was evaluated against carrageenan-induced hind paw edema model and reported in Table 3. Amongst all ten evaluated compounds, three compounds (**1e**, **3e**, and **3b**) showed considerable anti-inflammatory activity 79.35, 79.35, and 75.00%, respectively. Compounds **1e** and **3e** comprising of strong electron-donating hydroxyl (-OH) substituent on benzylidene elicited the maximal anti-inflammatory activity amongst the synthesized derivatives. Compounds (**3a**, **1c**, and **3c**) comprising of an electron-donating phenyl (**3a**) and methyl ($-CH_3$) substituent on benzylidene (**1c** and **3c**) exhibited an average reduction of 64.13, 59.78, and 57.61% of inflammation. Compounds (**1d** and **3d**) comprising of strong electron withdrawing substituents exhibited weak inhibitory activity (54.35, and 53.26%). The results thus reaffirm the anti-inflammatory potential of compounds (**1e** and **3e**).

Table 4 % Mean protection by AA-induced rat paw edema model

Compound	Mean protection[a] (%)
Control	–
Zileuton	66.15
1a	36.92
1b	41.53
1c	40.00
1d	43.07
1e	55.38
3a	47.69
3b	55.38
3c	50.76
3d	35.38
3e	58.46

All other compounds were administered at an equimolar oral dose relative to 10 mg kg^{-1} standard

[a]*Standard* zileuton (10 mg kg^{-1} p.o) in 0.3% CMC solution

Protection (%) was expressed as % edema inhibition of the tested compounds relative to % edema inhibition of standard

Arachidonic acid-induced rat paw edema

AA-induced rat paw edema is used extensively to evaluate the anti-inflammatory activity through LOX inhibition pathway. This model is more sensitive to observe the LOX than COX enzyme inhibition (DiMartino et al. 1987). The LOX inhibitors appreciably reduce the paw edema induced by AA. The results (Table 4) showed that synthesized compounds (**1a–1e** and **3a–3e**) exhibited anti-inflammatory activity against AA-induced rat paw edema. Compound **3e** and the standard zileuton considerably inhibit the AA-induced inflammation with the mean protection percentage of 58.46 and 66.15%, respectively. The test compounds

Table 5 The ulcerogenic activity of compound **3e**

Compounds	Ulcer index range (mean ± SEM)
3e	10.2 ± 1.4
Diclofenac	46.0 ± 4.1
Zileuton	52.0 ± 4.9

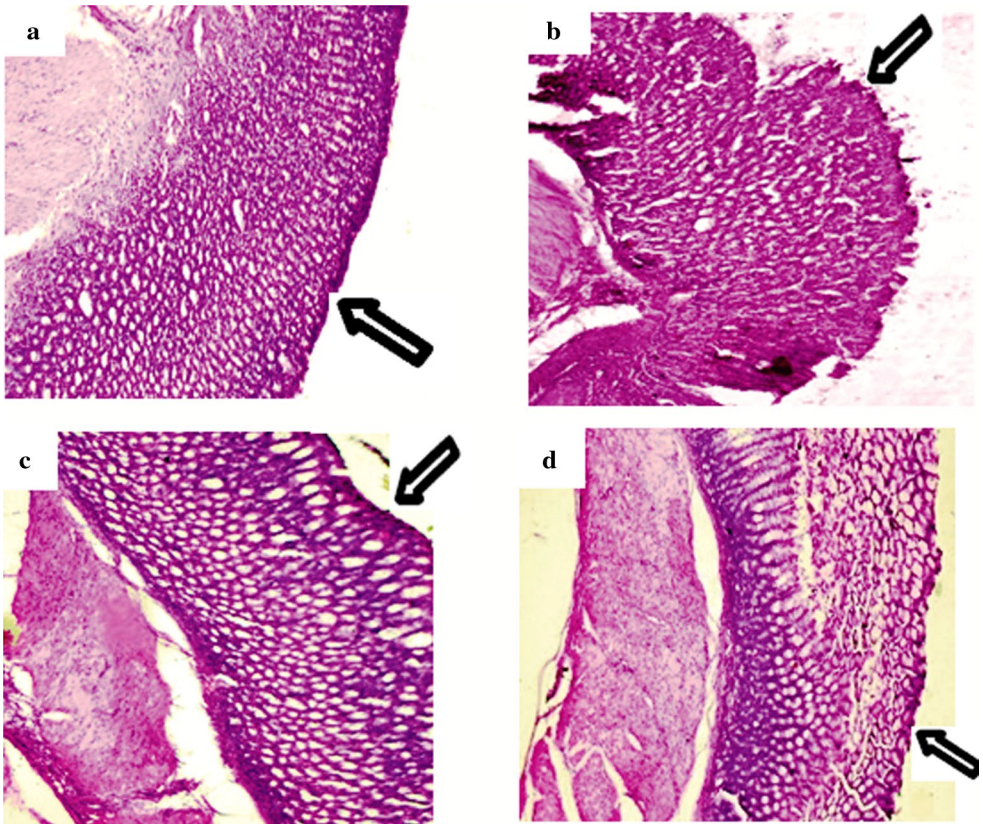

Fig. 2 Photomicrographs (10x magnification) of **a** control; **b** diclofenac; **c** Zileuton and **d** compound 3e-treated groups in rat stomach tissues (hematoxylin and eosin staining). Green arrow shows detachment of surface epithelium resulting in the formation of gastric lesions. Black arrow shows the normal stomach structure with less or no ulcer formation

Table 6 IC_{50} values of compounds **1e** and **3e**

Compounds	COX-1 IC_{50} (μM) ± SEM	COX-2IC_{50} (μM) ± SEM	LOX IC_{50} (μM) ± SEM	Type of inhibition	LOX Ki (μM)
1e	>50	>50	12.98 ± 0.17	nd[a]	nd[a]
3e	>50	>50	12.67 ± 0.24	Non-competitive	0.73
Celecoxib	6.70 ± 0.03	0.87 ± 0.04	nd[a]	nd[a]	nd[a]
Diclofenac	0.15 ± 0.01	0.05 ± 0.01	nd[a]	nd[a]	nd[a]
Zileuton	nd[a]	nd[a]	3.43 ± 0.04	Non-competitive	0.49
C06[b]	nd[a]	nd[a]	9.86 ± 0.02	Non-competitive	0.58
ST1098[c]	nd[a]	nd[a]	8.20 ± 0.02	Non-competitive	0.56

[a]Not determined

[b]Hofmann et al. 2012

[c]Barzen et al. 2012

(**1a–1e** and **3a–3e**) inhibited the formation of edema up to 35.38–58.46%. Based on the outcome of the study, mono-substituted electronegative (-OH) group on benzylidene of 4-thiazolone can be considered as a key marker in the determination of anti-inflammatory activity of *p*-substituted benzylidene 4-thiazolone derivatives. Our findings revealed that 5-benzylidene-4-thiazolones with substituted electronegative (-OH) groups are effective inhibitors of LOX enzyme.

Acute ulcerogenic studies

The most active compound (**3e**) and standard drugs (diclofenac and zileuton) were subjected to their ulcerogenic liabilities in rats. The results of ulcer index (UI) of the test compound and standard drugs are calculated and mentioned in Table 5. The study demonstrated that compound (**3e**) has minimal gastric insult compared to standard

drugs diclofenac and zileuton. Gastric mucosa lesion liability was evaluated and supported by histological evaluation (Fig. 2). These outcomes revealed that the test compound (**3e)** elicited less damage to the gastric mucosa compared to standard drugs.

In-vitro COX inhibition assay

In-vitro COX inhibition of compound (**1e** and **3e**) was performed on ovine COX-1 and human COX-2 enzymes using colorimetric enzyme immunoassay (EIA). Along with the compounds (**1e** and **3e**), the standard diclofenac and celecoxib were tested and results are reported in Table 6. The results suggested that compounds (**1e** and **3e)** have significantly lower inhibitory potential against COX-1 and COX-2 (COX-1; $IC_{50} > 50$ µM, COX-2; $IC_{50} > 50$ µM) compared to standard drugs diclofenac (COX-1; $IC_{50} = 0.15 \pm 0.01$ µM, COX-2; $IC_{50} = 0.05 \pm 0.01$ µM) and celecoxib (COX-1; $IC_{50} = 6.70 \pm 0.03$ µM, COX-2; $IC_{50} = 0.87 \pm 0.04$ µM).

In-vitro LOX inhibition assay

The active compounds (**1e** and **3e**) were evaluated against in vitro LOX enzyme to determine the respective IC_{50} values to ascertain their specificity. The results showed that compounds **1e** ($IC_{50} = 12.98 \pm 0.17$ µM) and **3e** ($IC_{50} = 12.67 \pm 0.24$ µM) have considerable lipoxygenase (LOX) enzyme inhibitory activity with standard zileuton ($IC50 = 3.43 \pm 0.04$ µM), **ST1098** ($IC50 = 8.20 \pm 0.02$ µM) and **C06** ($IC50 = 9.86 \pm 0.02$ µM), respectively (Table 6).

Enzyme kinetic studies

The Lineweaver–Burk plot was used to determine the type of enzyme inhibition. The active compound (**3e**) was evaluated for substrate-dependent enzyme kinetics (Fig. 3). In the presence or absence of inhibitor, different $1/V_{max}$ (y-intercept) values were obtained, and inhibition constant (K_i) was calculated (Table 6). The Lineweaver–Burk plot analysis suggested that compound **(3e)** is the non-competitive inhibitor.

Computational studies

Molecular docking study

The compounds (**1e** and **3e)** with effective in vitro LOX inhibitory activity were evaluated for in silico docking studies to measure the binding interactions at the active binding pocket of LOX enzyme (PDB Code: 3V99). The docking simulations were performed using the Glide-XP protocol in the Schrödinger software suite (Schrödinger, LLC, USA, 2016-1 Maestro 10.5.014). The compounds (**1e** and **3e)** showed to occupy the active binding pocket of the enzyme and are involved in the interactions with the active site amino acid residues (Fig. 4a, b).

Molecular dynamics simulations

Molecular dynamics simulations of compound **3e** with LOX enzyme (PDB Code: 3V99) was performed up to 50 ns time scale to predict the binding stability of the docked conformation. The results were analyzed using root mean square deviation (RMSD) and root mean square fluctuation (RMSF) protocols. The protein–ligand contacts during the entire simulation time scale were also analyzed.

The RMSD value revealed that initially up to 25 ns time scale, trajectories were unstable and showed several fluctuations. Stable trajectories were observed after 25 ns timescale with average fluctuation less than 1 Å (Fig. 5).

Further, root mean square fluctuations (RMSF) of active amino acid residues of the enzyme with compound **3e** exhibited stable movements (Supplementary Fig. S17).

The interactions of the ligand with protein play a significant role in the stability of the protein–ligand complex. The interaction pattern of compound **3e** with LOX enzyme was also evaluated (Supplementary Fig. S18). The results showed that amino acid residues Phe177, Thr364, Lys409, Ala410, Glu412, His432, and Leu607 contribute to strong hydrogen bonding interaction throughout the simulation timescale. The interactions observed in docking were also retained throughout the simulation run. The percentage of interaction by the interacting residue is analyzed and represented as a histogram in Fig. 6.

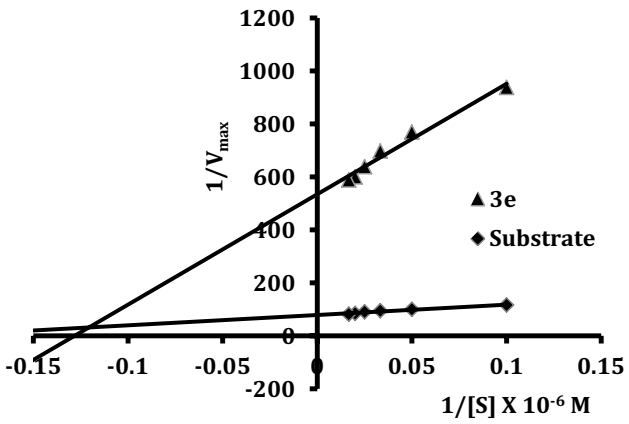

Fig. 3 In-vitro LOX enzyme kinetics showing the non-competitive type of inhibition by compound **3e**

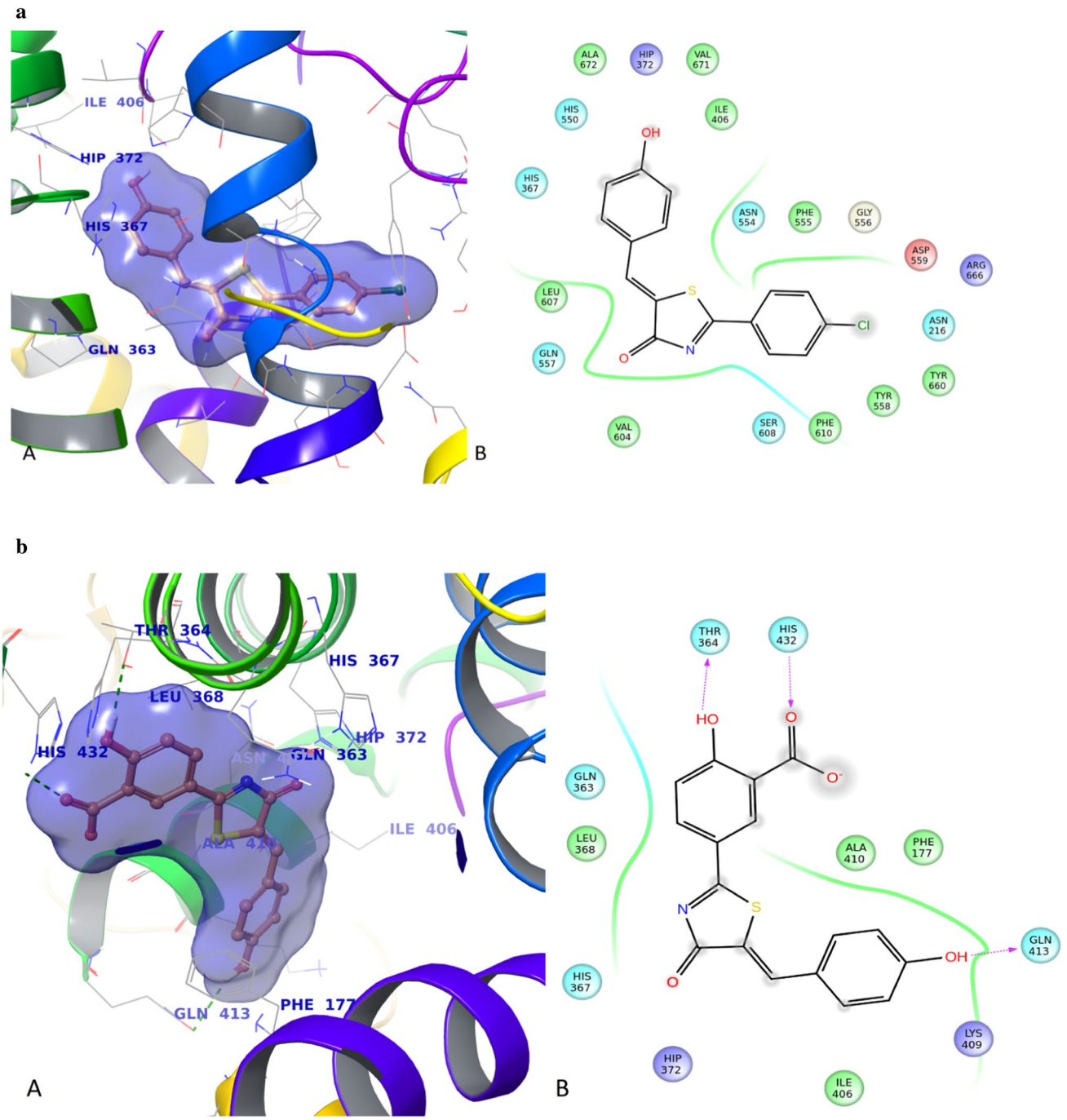

Fig. 4 **a** Binding mode of **1e** docked into the 'active site' of LOX enzyme. **b** Binding mode of **3e** docked into the 'active site' of LOX enzyme

In-silico ADME studies

The compound **3e** was also evaluated for drug likeliness characteristics using QikProp module of Schrödinger Suite. The results suggested that compound **3e** has more polar surface area and lower predicted partition coefficient values, compared to standards **C06** and **ST1098** (Table 7).

Conclusions

The synthesized compounds (**1e** and **3e**) exhibited potential anti-inflammatory activities against carrageenan and AA-induced rat paw edema models with a lesser ulcerogenic insult compared with standard drugs diclofenac and zileuton. The kinetic study of (**3e**) revealed a non-competitive type of inhibition. The strong electron-donating

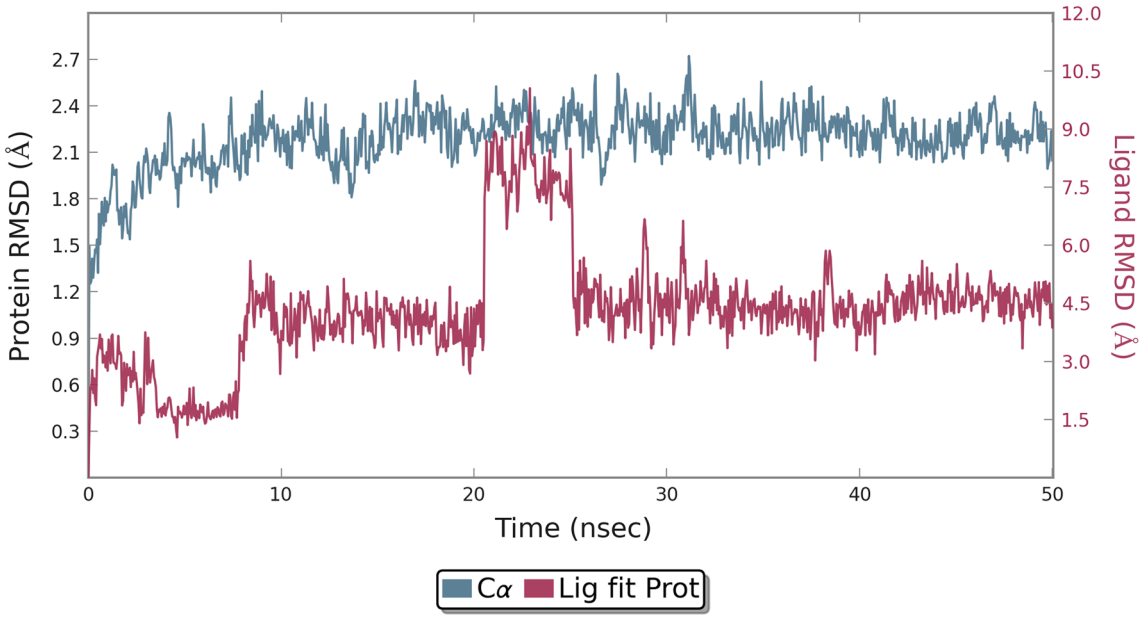

Fig. 5 RMSD graph of the compound (**3e**) and LOX enzyme complex for the period of 50 ns simulation

hydroxyl group on benzylidene of compound (**3e**) exhibited high mean protection against inflammation compared to compounds (**1a–1d** and **3a–3d**). The docking studies illustrated that compound (**3e**) has an excellent fit into the pocket of LOX enzyme with minimum energy compared with compound (**1e**), which might be attributed to better hydrogen bonding interaction of *p*-hydroxy benzylidene at 5th position and *o*-hydroxybenzoic acid at 2nd position of 4-thiazolone. Further, molecular dynamics studies confirmed that active site interaction of compound **(3e)** was stable throughout simulation timescale. With these findings, it can be postulated that the

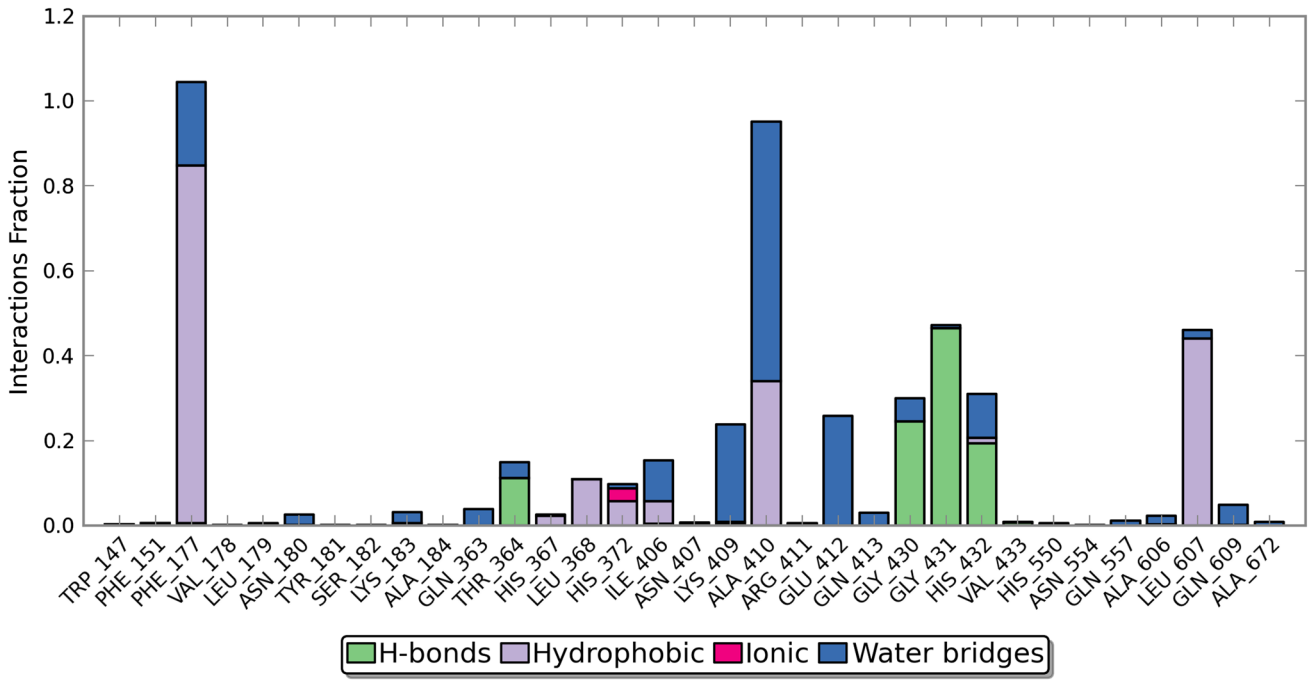

Fig. 6 Protein–ligand contacts through 50 ns simulation of compound **3e–LOX** enzyme

Table 7 Comparative QikProp analysis properties of compounds 3e, zileuton, C06, and ST1098

Code	SASA[a]	PSA[b]	DonorHB[c]	AcceptHB[d]	QPlogPC16[e]	QPlogPoct[f]	QPlogPo/w[g]
3e	581.1	132.7	2	6	11.8	17.8	1.9
Zileuton	447.7	73.5	3	3.7	8.4	14.6	0.9
C06	581.5	49.9	0	4.3	10.1	14.1	3.6
ST1098	574.11	49.9	0	4.3	10.5	14.1	3.8

[a]*SASA* Total solvent accessible surface area in square angstroms using a probe with a 1.4 Å radius (range 300–1000 Å)

[b]*PSA* Van der Waals surface area of polar nitrogen and oxygen atoms (range 7–200)

[c]*DonorHB* H-bond donors (range 0–6)

[d]*AcceptHB* H-bond acceptors (range 2–20)

[e]*QPlogPC16* predicted log of hexadecane/gas partition coefficient (range 4–18)

[f]*QPlogPoct* predicted log of octanol/gas partition coefficient (range 8–43)

[g]*QPlogPo/w* predicted log of octanol/water partition coefficient (range 2–6)

5-benzylidene-2-phenyl-4-thiazolones moiety is an essential pharmacophore necessary to elicit the inhibitory activity against LOX enzyme along with the lesser ulcerogenic liability.

Acknowledgements The authors gratefully acknowledge Indian Institute of Technology (BHU) for providing financial assistance through Institute Research Project (IRP) scheme and Design Innovation Center (DIC) scheme. Grant No. IIT (BHU)/R&D/IRP/2015-16/3471/L and Grant No. DIC-IIT(BHU)/L-11, respectively. The authors are also thankful to Department of Health Research, Ministry of Health and Family Welfare for providing the Young Scientist Project in newer areas of Drugs Chemistry (DHR/HRD/YS-15-2015-16).

References

Ali AM, Saber GE, Mahfouz NM, El-Gendy MA, Radwan AA, Hamid MA (2007) Synthesis and three-dimensional qualitative structure selectivity relationship of 3, 5-disubstituted-2, 4-thiazolidinedione derivatives as COX2 inhibitors. Arch Pharm Res 30:1186–1204. https://doi.org/10.1007/BF02980259

Allaj V, Guo C, Nie D (2013) Non-steroid anti-inflammatory drugs, prostaglandins, and cancer. Cell Biosci 3:8. https://doi.org/10.1186/2045-3701-3-8

Aparoy P, Kumar Reddy K, Reddanna P (2012) Structure and ligand based drug design strategies in the development of novel 5-LOX inhibitors. Curr Med Chem 19:3763–3778. https://doi.org/10.2174/092986712801661112

Banerjee AG, Das N, Shengule SA, Srivastava RS, Shrivastava SK (2015) Synthesis, characterization, evaluation and molecular dynamics studies of 5, 6–diphenyl–1, 2, 4–triazin–3 (2H)–one derivatives bearing 5–substituted 1, 3, 4–oxadiazole as potential anti–inflammatory and analgesic agents. Eur J Med Chem 101:81–95. https://doi.org/10.1016/j.ejmech.2015.06.020

Banerjee AG, Das N, Shengule SA, Sharma PA, Srivastava RS, Shrivastava SK (2016) Design, synthesis, evaluation and molecular modelling studies of some novel 5, 6-diphenyl-1, 2, 4-triazin-3 (2H)-ones bearing five-member heterocyclic moieties as potential COX-2 inhibitors: A hybrid pharmacophore approach. Bioorg Chem 69:102–120. https://doi.org/10.1016/j.bioorg.2016.10.003

Barreiro EJ, Fraga CA, Miranda AL, Rodrigues CR (2002) A química medicinal de *N*-acilidrazonas: Novos compostos-protótipos de fármacos analgésicos, antiinflamatórios e anti-trombóticos. Quim Nova 25:129–148. https://doi.org/10.1590/S0100-40422002000100022

Barzen S, Rödl CB, Lill A, Steinhilber D, Stark H, Hofmann B (2012) Synthesis and biological evaluation of a class of 5-benzylidene-2-phenyl-thiazolinones as potent 5-lipoxygenase inhibitors. Bioorg Med Chem 20:3575–3583. https://doi.org/10.1016/j.bmc.2012.04.003

Bekhit AA, Fahmy HT, Rostom SA, Bekhit AE-DA (2010) Synthesis and biological evaluation of some thiazolylpyrazole derivatives as dual anti-inflammatory antimicrobial agents. Eur J Med Chem 45:6027–6038. https://doi.org/10.1016/j.ejmech.2010.10.001

Berger W, De Chandt M, Cairns C (2007) Zileuton: clinical implications of 5-lipoxygenase inhibition in severe airway disease. Int J Clin Pract 61:663–676. https://doi.org/10.1111/j.1742-1241.2007.01320.x

Carter BZ, Wiseman AL, Orkiszewski R, Ballard KD, Ou C-N, Lieberman MW (1997) Metabolism of leukotriene C4 in γ-glutamyl transpeptidase-deficient mice. J Biol Chem 272:12305–12310. https://doi.org/10.1074/jbc.272.19.12305

Deep A, Jain S, Sharma PC (2010) Synthesis and anti-inflammatory activity of some novel biphenyl-4-carboxylic acid 5-(arylidene)-2-(aryl)-4-oxothiazolidin-3-yl amides. Acta Pol Pharm 67:63–67

DiMartino M, Campbell G, Wolff C, Hanna N (1987) The pharmacology of arachidonic acid-induced rat paw edema. Inflamm Res 21:303–305. https://doi.org/10.1007/BF01966498

Drazen JM, Israel E, O'byrne PM (1999) Treatment of asthma with drugs modifying the leukotriene pathway. N Engl J Med 340:197–206. https://doi.org/10.1056/NEJM199901213400306

Franke L, Hofmann B, Schneider G, Steinhilber D (2009) Neue Inhibitoren der 5-lipoxygenase und deren Verwendungen New inhibitors of 5-lipoxygenase and their uses. In: Patent G (ed) German Patent. Johann Wolfgang Goethe-Universität Frankfurt am Main, German

Gilbert NC, Bartlett SG, Waight MT, Neau DB, Boeglin WE, Brash AR, Newcomer ME (2011) The structure of human 5-lipoxygenase. Science 331:217–219. https://doi.org/10.1126/science.1197203

Hofmann B, Franke L, Proschak E, Tanrikulu Y, Schneider P, Steinhilber D, Schneider G (2008) Scaffold-hopping cascade yields potent inhibitors of 5-lipoxygenase. ChemMedChem 3:1535–1538. https://doi.org/10.1002/cmdc.200800153

Hofmann B, Barzen S, Rödl CB, Kiehl A, Borig J, Živković A, Stark H, Schneider G, Steinhilber D (2011) A class of 5-benzylidene-2-phenylthiazolinones with high potency as direct 5-lipoxygenase inhibitors. J Med Chem 54:1943–1947. https://doi.org/10.1021/jm101165z

Hofmann B, Rödl C, Kahnt A, Maier T, Michel A, Hoffmann M, Rau O, Awwad K, Pellowska M, Wurglics M (2012) Molecular pharmacological profile of a novel thiazolinone-based direct and selective 5-lipoxygenase inhibitor. Br J Pharmacol 165:2304–2313

Liang Z-Q, Yi L, Chen K-Q, Ye S (2016) N-heterocyclic carbene-catalyzed [3 + 4] annulation of enals and alkenyl thiazolones: enantioselective synthesis of thiazole-fused ε-lactones. J Org Chem 81:4841–4846. https://doi.org/10.1021/acs.joc.6b00313

Lineweaver H, Burk D (1934) The determination of enzyme dissociation constants. J Am Chem Soc 56:658–666. https://doi.org/10.1021/ja01318a036

Martel-Pelletier J, Lajeunesse D, Reboul P, Pelletier J (2003) Therapeutic role of dual inhibitors of 5-LOX and COX, selective and non-selective non-steroidal anti-inflammatory drugs. Ann Rheum Dis 62:501–509. https://doi.org/10.1136/ard.62.6.501

Murphy RC, Gijón MA (2007) Biosynthesis and metabolism of leukotrienes. Biochem J 405:379–395. https://doi.org/10.1042/BJ20070289

Ottana R, Maccari R, Barreca ML, Bruno G, Rotondo A, Rossi A, Chiricosta G, Di Paola R, Sautebin L, Cuzzocrea S (2005) 5-Arylidene-2-imino-4-thiazolidinones: design and synthesis of novel anti-inflammatory agents. Bioorg Med Chem 13:4243–4252. https://doi.org/10.1016/j.bmc.2005.04.058

Pergola C, Werz O (2010) 5-Lipoxygenase inhibitors: a review of recent developments and patents. Expert Opin Ther Pat 20:355–375. https://doi.org/10.1517/13543771003602012

Pradelles P, Grassi J, Maclouf J (1985) Enzyme immunoassays of eicosanoids using acetylcholine esterase as label: an alternative to radioimmunoassay. Anal Chem 57:1170–1173. https://doi.org/10.1021/ac00284a003

Qiu J, Stevenson SH, O'Beirn MJ, Silverman RB (1999) 2, 6-difluorophenol as a bioisostere of a carboxylic acid: bioisosteric analogues of γ-aminobutyric acid. J Med Chem 42:329–332. https://doi.org/10.1021/jm980435l

Reddy KK, Rajan VKV, Gupta A, Aparoy P, Reddanna P (2015) Exploration of binding site pattern in arachidonic acid metabolizing enzymes, cyclooxygenases and lipoxygenases. BMC Res Notes 8:152. https://doi.org/10.1186/s13104-015-1101-4

Rossi A, Pergola C, Koeberle A, Hoffmann M, Dehm F, Bramanti P, Cuzzocrea S, Werz O, Sautebin L (2010) The 5-lipoxygenase inhibitor, zileuton, suppresses prostaglandin biosynthesis by inhibition of arachidonic acid release in macrophages. Br J Pharmacol 161:555–570. https://doi.org/10.1111/j.1476-5381.2010.00930.x

Sandmeyer T (1884) Ueber die Ersetzung der Amid-gruppe durch Chlor, Brom und Cyan in den aromatischen Substanzen. Eur J Inorg Chem 17:2650–2653. https://doi.org/10.1002/cber.188401702202

Schneider G, Steinhilber D, Franke L, Hofmann B (2009) 5-arylalkylidene-2-arylalkyl-thiazol-4-one derivatives as inhibitors of 5-lipoxygenase and uses thereof. In: Patent W (ed) World Patent. Johann Wolfgang Goethe-Universität, Frankfurt Am Main

Scholz M, Ulbrich HK, Soehnlein O, Lindbom L, Mattern A, Dannhardt G (2009) Diaryl-dithiolanes and-isothiazoles: COX-1/COX-2 and 5-LOX-inhibitory, OH scavenging and anti-adhesive activities. Bioorg Med Chem 17:558–568. https://doi.org/10.1016/j.bmc.2008.11.074

Shrivastava SK, Srivastava P, Bendresh R, Tripathi PN, Tripathi A (2017) Design, synthesis, and biological evaluation of some novel indolizine derivatives as dual cyclooxygenase and lipoxygenase inhibitor for anti-inflammatory activity. Bioorg Med Chem. https://doi.org/10.1016/j.bmc.2017.06.027

Srivastava P, Vyas VK, Variya B, Patel P, Qureshi G, Ghate M (2016) Synthesis, anti-inflammatory, analgesic, 5-lipoxygenase (5-LOX) inhibition activities, and molecular docking study of 7-substituted coumarin derivatives. Bioorg Chem 67:130–138. https://doi.org/10.1016/j.bioorg.2016.06.004

Szelenyi I, Thiemer K (1978) Distention ulcer as a model for testing of drugs for ulcerogenic side effects. Arch Toxicol 41:99–105. https://doi.org/10.1007/BF00351774

Tsurumi K, Kyuki K, Niwa M, Kokuba S, Fujimura H (1986) Pharmacological investigations of the new antiinflammatory agent 2-(10,11-dihydro-10-oxodibenzo[b,f]thiepin-2-yl)propionic acid. 1st communication: inhibitory effects of rat paw edema. Arzneimittelforschung 36:1796–1800

Wenzel SE, Kamada AK (1996) Zileuton: the first 5-lipoxygenase inhibitor for the treatment of asthma. Ann Pharmacother 30:858–864. https://doi.org/10.1177/106002809603000725

Winter CA, Risley EA, Nuss GW (1962) Carrageenin-induced edema in hind paw of the rat as an assay for antiinflammatory drugs. Proc Soc Exp Biol Med 111:544–547. https://doi.org/10.3181/00379727-111-27849

Zaitsu M, Hamasaki Y, Matsuo M, Ichimaru T, Fujita I, Ishii E (2003) Leukotriene synthesis is increased by transcriptional up-regulation of 5-lipoxygenase, leukotriene A4 hydrolase, and leukotriene C4 synthase in asthmatic children. J Asthma 40:147–154. https://doi.org/10.1081/JAS-120017985

Zayed E, Elbannany A, Ghozlan S (1985) Studies on thiazolin-4-one: synthesis of some pyrano [2, 3-b]-thiazole derivatives. Pharmazie 40:194–196